Conclusion: Augmenting whole liver scRNA seq with spatial transcriptome analysis, is a novel approach to identify cell populations and pathways specific to the damaged peribiliary area. Using this approach we demonstrated that CCL24 regulates cholestatic, inflammatory and fibrotic liver damage, and its underling mechanisms. Understanding the underling mechanisms of CCL24 blockade and its ability to prevent liver injury in animal supports its role in PSC and its potential beneficial effect for PSC patients.

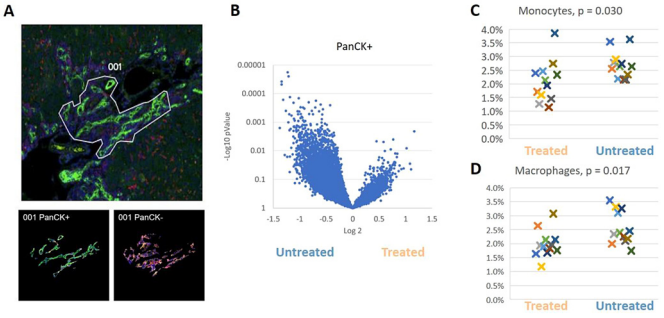

OS023

T regulatory cells promote bile duct regeneration through modulating ductular reaction in a model of cholestatic liver injury

Naruhiro Kimura[1,2,3], Gareth Hardisty[1], Atsunori Tsuchiya[3], Shuji Terai[3], David Withers[2], Wei-Yu Lu[1,2]. [1]*University of Edinburgh, Centre for Inflammation Research, Edinburgh, United Kingdom;* [2]*University of Birmingham, Institute of Immunology and Immunotherapy, Birmingham, United Kingdom;* [3]*Niigata University, Division of Gastroenterology and Hepatology, Niigata, Japan*
Email: w.y.lu@ed.ac.uk

Background and aims: Reduced regulatory T cells (Tregs) and increased bile duct senescence are observed in primary sclerosing cholangitis (PSC) patients, with the degree of cholangiocyte senescence linking to disease severity and prognosis. Cholangiocytes can act as facultative liver progenitor cells through ductular reaction during extensive liver damage, whether this process is impaired during PSC remains to be investigated. The role of Tregs in modulating tissue resident progenitor cells have been shown in multiple organs, but this remains unclear in the context of liver regeneration. We aim to use transgenic murine models to investigate the cause of reduced Tregs in the liver and whether the lack of Tregs in the liver affect bile duct regeneration and senescence.
Method: Foxp3^{GFP}DTR transgenic mice were used to reduce Tregs number in a dose dependant manner. 50% of Tregs were depleted to avoid triggering systematic autoimmunity whilst cholestatic liver injury was induced by the feeding of 3, 5-diethoxycarbonyl-1, 4-dyhydrocollidine (DDC) diet and compared to the control group with intact Tregs population. We generated the Foxp3^{GFPCreERT}tdTom^{loxSTOPlox} mice to investigate Tregs stability. Tamoxifen was injected intraperitoneally to induce tdTom expression in Foxp3 Tregs and cell fate was investigated after DDC diet to determine Tregs stability. CD4 T-cells were isolated and co-cultured with intrahepatic cholangiocytes organoids to confirm the effect of CD4 T-cells on cholangiocytes.
Results: Mice with reduced Tregs have a lower tolerance to the feeding of DDC diet, with rapid weight loss and two times higher periportal fibrosis than the control group. Histological findings showed that the reduction in Tregs decrease the magnitude of Ck19^{+} ductular reaction by 30%. A two-fold increase in Ck19+p21+ senescing cholangiocytes was observed in the group with reduced Tregs after DDC induced liver injury. Transcriptional analysis of liver tissue revealed downregulation of *Yap1*, *Sox9* and *Ctgf*, suggesting the Yap pathway is affected following Tregs reduction. This is further confirmed with immunohistochemistry showing a two-fold reduction in the number of Yap and Sox9 expressing Ck19+ cholangiocytes. The Foxp3 fate mapping experiments showed that the labelled Tregs population reduces Foxp3 expression after DDC diet indicating that the stability of Tregs decreases during liver injury.
Conclusion: Our results demonstrated that the role of Tregs in promoting bile duct regeneration by modulating ductular reaction through the Hippo-Yap pathway. Furthermore, the observation that Foxp3 Tregs become unstable in an injured microenvironment in mice may explain the lack of Tregs seen in PSC patients. These show the potential of using Tregs to promote liver regeneration but also highlights the stability of Tregs should be taken into consideration when designing cell based Tregs therapy.

OS024

Deep learning for automatic diagnosis and morphologic characterisation of malignant biliary strictures using digital cholangioscopy: a pilot study

Miguel Mascarenhas[1], João Afonso[1], Tiago Ribeiro[1], Ana Santos[1], Hélder Cardoso[1], João Pedro Sousa Ferreira[2], Filipe Vilas-Boas[1], Pedro Pereira[1], Guilherme Macedo[1]. [1]*Centro Hospitalar Universitário de São João, Department of Gastroenterology, Porto, Portugal;* [2]*Faculdade de Engenharia da Universidade do Porto, Department of Mechanical Engineering, Porto, Portugal*
Email: miguelmascarenhassaraiva@gmail.com

Background and aims: Patients with indeterminate biliary strictures (BS) pose a significant diagnostic challenge. Digital cholangioscopy (DC) has enabled morphologic characterization as well as the performance of visually guided biopsies. However, the diagnostic yield of DC remains suboptimal, and the visual characterization of these lesions has significant interobserver variability. Recently, the development of artificial intelligence (AI) algorithms, particularly convolutional neural networks (CNNs) for interpretation of endoscopic images has generated intense interest. We aimed to develop a CNN-based system for simultaneous automatic detection of malignant BS in D-SOC images and identification of three morphologic features: nodules (NN), papillary projections (PP) and tumor vessels (TV).
Method: We developed and validated a CNN based on DC images (Spyglass DS II, Boston Scientific, USA). Each frame was labeled as normal/benign finding or as a malignant lesion if definite histologic evidence of biliary malignancy was available. Moreover, we evaluated the performance of the CNN for the detection of morphologic features associated with histology-proved biliary malignancy: NN, PP, and TV. The image dataset was split for constitution of training and validation datasets. The performance of the CNN was measured by calculating the accuracy, area under the curve (AUC), sensitivity, specificity, positive and negative predictive values (PPV and NPV, respectively).
Results: We included 23 595 images from 125 patients (20719 of malignant BS and 2876 of normal or benign findings). The model had a sensitivity of 98.9%, a specificity of 97.7% and an overall accuracy of 98.7%. The AUC was 1.00.
Additionally, the model comprised 2876 images of NN, 1675 images showing PP, and 4153 images of YV. The accuracy for the automatic detection of each of these features was, respectively, 96.9%, 96.1%, and 91.5%.
Conclusion: We developed a combined CNN for automatic detection of malignant BS as well as the automatic identification of morphologic features associated with increased probability of malignancy. The application of AI models to DC may increase its diagnostic yield for patients with indeterminate BS. Furthermore, accurate real-time automatic identification of features associated with increased probability of malignancy may help to guide biopsies, thus increasing their rentability.

Table 1: Performance metrics of the combined convolutional neural network

	Malignant strictures (vs. normal/benign findings)	NN (vs normal/other findings)	PP (vs normal/ other findings)	TV (vs normal/ other findings)
Sensitivity	98.9%	96.1%	98.2%	85.7%
Specificity	97.7%	98.9%	94.8%	100%
PPV	99.7%	99.5%	91.7%	100%
NPV	92.8%	91.4%	98.9%	82.5%
Accuracy	98.7%	96.9%	96.1%	91.5%
AUC	0.987	1.000	1.000	1.00

Abbreviations; PPV-positive predictive value; NPV-negative predictive value; AUC-area under the curve.

Non-invasive assessment/treatment and liver related outcomes in NAFLD/ALD

OS025

Non-invasive fibrosis scores as prognostic biomarkers of liver events, cardiovascular events and all-cause mortality in people with obesity and/or type 2 diabetes in the UK: a longitudinal cohort study

Quentin Anstee[1,2], Tina Landsvig Berentzen[3], Louise Nitze[3], Maximilian Jara[3], Mette Kjaer[3], Kamal Kant Mangla[3], Jens M. Tarp[3], Kamlesh Khunti[4]. *[1]Translational and Clinical Research Institute, Faculty of Medical Sciences, Newcastle University, Newcastle Upon Tyne, United Kingdom; [2]Newcastle NIHR Biomedical Research Centre, Newcastle Upon Tyne Hospitals NHS Trust, Newcastle Upon Tyne, United Kingdom; [3]Novo Nordisk A/S, Søborg, Denmark; [4]Diabetes Research Centre, University of Leicester, Leicester General Hospital, Leicester, United Kingdom*

Email: quentin.anstee@ncl.ac.uk

Background and aims: Progression of non-alcoholic steatohepatitis to cirrhosis may lead to life-threatening liver-related complications, increased liver-specific and all-cause mortality and cardiovascular (CV) disease. An important predictor of severe outcomes is biopsy-confirmed liver fibrosis, but biopsies are not scalable outside of specialist practice. This real-world study investigated the prognostic utility of six non-invasive fibrosis scores on clinical outcomes in patients with obesity and/or type 2 diabetes (T2D) seen in routine general practice.

Method: In a longitudinal cohort design, patients ≥18 years with obesity and/or T2D, ≥1 fibrosis score calculable from the UK Clinical Practice Research Datalink (CPRD) after 1 January 2001, no alcohol-related disorders and/or other chronic liver diseases in Hospital Episodes Statistics (HES) and/or no prescriptions of drugs inducing liver disease in CPRD were included. Patients were followed from inclusion date until time of first clinical outcome event (liver-related hospitalisation or death [liver event], CV hospitalisation or death [CV event] or all-cause death) recorded in HES or Office for National Statistics Death Registration, database migration, 10 years' follow-up or 1 January 2020, whichever came first. Fibrosis-4 Index (FIB4), the score of focus, was categorised as low (<1.30), indeterminate (1.30–2.67) or high (>2.67) risk. Cumulative incidence functions were calculated and hazard ratios (HRs) estimated using Cox proportional hazards models with calendar time as underlying timescale.

Results: In total, 44 481 eligible patients (46% male, median age 58.8 years) had measures available for FIB4 calculation. There were 979 liver events, of which ascites (n = 412), cirrhosis (n = 201) and gastro-oesophageal varices (n = 160) were most common. The risk of an incident liver event was highest in the first years after FIB4 measurement in the high FIB4 group and relatively constant over time in the other two groups (Figure). The incidences of a liver event, CV event and death in the high FIB4 group were 15%, 33% and 61%, respectively. Patients in the indeterminate and high FIB4 groups were at greater risk of liver events vs the low-risk group (HR 2.81 [95% confidence interval 2.43, 3.26] and 18.42 [15.67, 21.65], respectively). An increased risk was also seen for CV events and all-cause mortality in these groups. HRs remained higher for the high vs low FIB4 group after adjustment for sex and age. For the other scores, risk of an outcome event was also elevated for patients with a high vs low score.

Cumulative incidence plots for liver events, cardiovascular events and mortality according to Fibrosis-4 Index (FIB4) in the population with obesity and/or type 2 diabetes

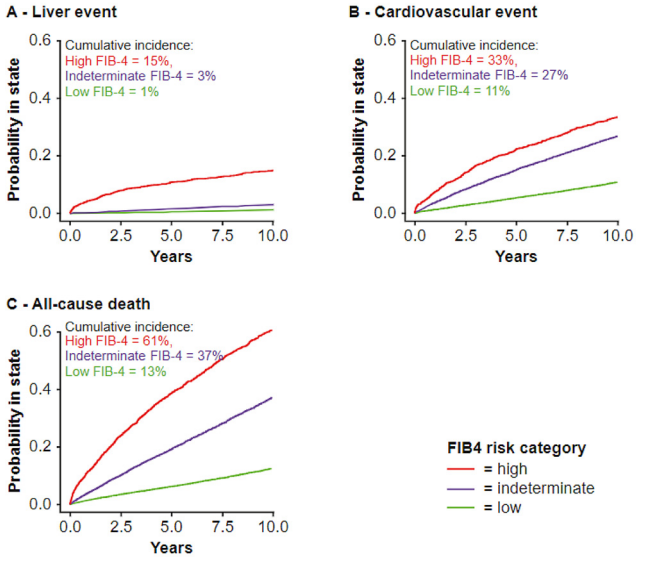

Percentage risks are for 10 years' follow-up. Event risks plotted as Aalen-Johansen cumulative incidence functions, with all-cause mortality included as a competing risk factor in plots of liver and cardiovascular events.

Conclusion: In this real-world population of patients with obesity and/or T2D, and no other clinically recognised liver disease, the risk of a clinical event was significantly higher in patients with high vs low FIB4 score, highlighting the prognostic potential of FIB4 (and other non-invasive fibrosis scores) in this population.